Published Online First: September, 2024
https://doi.org/10.21123/bsj.2024.9381
P-ISSN: 2078-8665 - E-ISSN: 2411-7986
Baghdad Science Journal

Chlorophyll Concentration and Its Impact on Electrospun Acrylic Nanofibers

Zainab Jassim , ***Mohammed Akraa****

Department of Physics, College of Education for Pure Sciences, University of Babylon, Hillah, Iraq.
*Corresponding Author.

Received 11/09/2023, Revised 02/02/2024, Accepted 04/02/2024, Published Online First 20/09/2024

Abstract

This study explores the properties of electrospun nanofibers of polymethyl methacrylate (PMMA) blended with chlorophyll, which have potential applications in photovoltaic manufacturing. Different chlorophyll concentrations (0, 0.05, 0.1, 0.15, 0.2, and 0.25 wt.%) were added to the electrospinning solutions of PMMA and acetone. After the electrospinning procedure and the evaporation of acetone, the fibers contained the chlorophyll concentrations of (0, 0.31, 0.63, 0.94, 1.25, and 1.56 wt.%). Rheology, Fourier Transformation Infrared Radiation, scanning electron microscopy, and UV-vis spectroscopy characterized the resulting fibers. The results revealed that chlorophyll increased the solution's viscosity and decreased the nanofibers' diameter up to 0.8 wt.%. The most uniform nanofibers were obtained at 0.31 wt.% chlorophyll, with an average diameter of 11.66 ± 7.3 nm. Higher chlorophyll concentrations led to larger and more irregular nanofibers and increased band gap. Chlorophyll concentrations above 1 wt.% produced undesirable fibers with beads. The study determined the optimal range of chlorophyll concentration for PMMA nanofibers (0-0.8 wt.%) and investigated the effect of chlorophyll on the viscosity, diameter, band gap, and morphology of the nanofibers. The study provides useful information for researchers and developers who want to use PMMA/chlorophyll nanofibers for various purposes.

Keywords: Chlorophyll Pigment, Electrospinning, Electrospun Nanofiber, Polymer Melts, Polymer Solutions.

Introduction

Electrospinning is a versatile technique for fabricating nanofibers from a variety of polymeric materials. It has been used to produce nanofibers from both synthetic and natural polymers, as well as blends of the two. Blending natural polymers with synthetic polymers can offer several advantages, such as improved mechanical properties, biodegradability, and biocompatibility.

Natural pigments and materials, such as chlorophyll, carotenoids, and lignin, can also be blended with polymers to produce electrospun nanofibers with unique properties. For example, chlorophyll-blended nanofibers have been shown to have photocatalytic activity, while lignin-blended nanofibers have been shown to have enhanced mechanical strength and barrier properties [1].

Electrospun nanofibers of blend polymer/natural pigment or material have a wide range of potential applications, including electrospun PMMA/chlorophyll nanofibers, which could be used to develop new types of solar cells that are more efficient and durable [1].Electrospun

Published Online First: September, 2024
https://doi.org/10.21123/bsj.2024.9381
P-ISSN: 2078-8665 - E-ISSN: 2411-7986
Baghdad Science Journal

nanofibers can be used to develop food-packaging materials that are biodegradable, antimicrobial, and have improved barrier properties. That can occur by blending some natural additives such as Fe_2O_3 with a polymer matrix[2,3]. Likewise, electrospun nanofibers of blend can be used to develop various biomedical applications, such as wound dressings, drug delivery systems, and tissue engineering scaffolds [4,5]. Moreover, this electrospinning production can be applied as an environmental remediation. This kind of fiber, which includes a blend of polymer/natural pigment or material such as biochar can be used to develop environmental remediation materials, such as filters for water and air purification [6,7].

Ince Yardimci et al.[8] investigated the electrospinning of polyacrylonitrile (PAN) nanofibers containing chlorophyll and their application for photocatalytic degradation of methylene blue (MB). The chlorophyll-loaded PAN nanofibers exhibit enhanced photocatalytic activity for MB degradation under visible light irradiation. Wang et al.[9] report the preparation and characterization of chlorophyll-loaded electrospun poly(methyl methacrylate) (PMMA) nanofibers and their application as an oxygen carrier. Maliszewska and Czapka . [10] investigate the antimicrobial activity of electrospun PMMA nanofibers incorporating chlorophyll-loaded liposomes. Liu et al.[11] report the fabrication of electrospun PAN/chlorophyll nanofiber mats and their application for photocatalytic degradation of dyes. The PAN/chlorophyll nanofiber mats exhibit enhanced photocatalytic activity for the degradation of various dyes under visible light irradiation. Cao et al.[12] investigated the preparation of chlorophyll-loaded electrospun PVA nanofibers for photocatalytic degradation of organic pollutants in wastewater. The PVA nanofibers containing chlorophyll demonstrate increased photocatalytic activity for organic pollutant degradation under visible light.

The research study aimed to examine the effect of chlorophyll concentration on the physical properties of the PMMA matrix. The results indicate that an optimal amount of chlorophyll can prevent the development of undesired structures in electrospun fibers. Such defects can reduce the toughness, porosity, and surface area of fibers during the electrospinning process [4.] To optimize fiber outcomes, several factors need to be managed and balanced, including drum rolling speed, the distance between the syringe needle and collector drum applied voltage, circulated aeration, temperature, moisture, and flow rate speed of the injection, an outer diameter of the syringe, syringe material, and applied fluid concentration. Overcoming these challenges requires patience, accurate observation, and experience. Measuring the thickness of electrospun fibers can be challenging, nevertheless SEM imaging technique offers the best way to do so.

Overall, this study provides new insights into the relationship between chlorophyll concentration and the properties of electrospun PMMA/chlorophyll nanofibers, which can be used to optimize the production of these materials for specific applications.

Natural chlorophyll occupies the first degree among the most natural pigments abundant and significant. This pigment offers an essential chemical structure for the process of photosynthesis in cooperation with the other molecules that are from so-called accessory pigments. They are located within membrane-spanning proteins for collecting solar energy [13]. Chlorophyll along with these accessory pigments presents the required chromophore to absorb all the visible light wavelengths. The energy conversion process that is carried out by the identities of photosynthesis that involve chlorophyll, chloroplasts, photosystems, etc occurs with a high efficiency of quantum and energy yield approaching one hundred percent. The stated property qualifies chlorophyll to be an auspicious nominee for photovoltaic appliances. The high imitation of the electrospun nanofibers to the biomolecular surrounding of the photosystems and pigments makes it a great candidate for the creation of fibers of photovoltaic instruments by the biology of herbs [14]. The electrospinning method is immensely creative in producing polymer fibers of diameter ranging from some microns to 10s nanometers. The mechanism of spinning relies on the electric attraction effect induced by an applied high voltage when injecting a solution of the polymer. The great benefits of this method are affordability, and harry production of nanofibers. The solubility of the additive material in the matrix material is a substantial condition for achieving a high-quality electrospinning process. However, the possibility of yielding coaxial nanofibers composed of more than one phase has been established [13.]

Published Online First: September, 2024
https://doi.org/10.21123/bsj.2024.9381
P-ISSN: 2078-8665 - E-ISSN: 2411-7986
Baghdad Science Journal

The absorption degree of a matter is well defined through the linear coefficient of absorption (α), which refers to the relative number of absorbed photons per unit-displaced distance (cm^{-1}) of a matter. This physical quantity is based on the incident photon energy and band gap of an absorber (Eg) [15]. The absorber thickness equals to the reciprocal value of its own absorption coefficient value absorb the rate of sixty-three percent out of the total number of the interacted photons. A material is considered transparent, whenever the value of its band gap is greater than the energy of the interacting photon. The absorption coefficient appears by the following relationship [15]:

$$\alpha = \frac{2.303*A}{t} \quad \ldots\ldots\ldots\ldots\ldots\ldots\ldots\ldots\ldots\ldots\ldots\ldots 1$$

Wherein, t is the thickness of the absorber, A is the absorbance. Based on the calculation of the linear absorption coefficient, the obtaining of band gap is potential through Eq. 2 [15]:

$$(\alpha h\nu)^m = D\left(h\nu - E_g\right) \quad \ldots\ldots\ldots\ldots\ldots\ldots\ldots \quad 2$$

Where h is Planck's constant, ν is the frequency, and D is a constant depending on the transition probability. Index m is an exponential constant that describes the optical absorption course. When the electronic transition is both direct and allowed then it equals two. If the electronic transition is allowed but indirect then, m equals half. For the forbidden electronic transition, m equals two third and one-third for the direct and indirect transitions, respectively. The majority of the kinds of literature [16] did not agree on the subject of specifying the amount of absorption coefficient. On the other side, literature [17] refers to the fact that the slope of the plot *log(α)* versus *log(hν)* represents the value of index *m*. broadly, the value of index m is obtained by choosing the best linear graph of $(\alpha h\nu)^m$ against $log(h\nu)$ [18]. The method of Tauc's plot offers a feasible style for extrapolating the value of the band gap through the crossing of the linear part of the curve with the *hν* axis.

In this work, six samples of electrospun nanofibers were prepared. The natural pigment of chlorophyll was added at different concentrations to the matrix polymer PMMA to prepare the polymer solutions of the blend. The rheological properties are measured and analyzed, sec. 3.1. The micro-nanofiber samples with chlorophyll, were deposited on aluminum foils and glass substrates by using an electrospinning technique. Scanning and analyzing (by using ImageJ software, Version 1.53t 24 August 2022(upgrade)) of the electrospun structures of SEM images were achieved, sec. 3.2. In addition to the UV-Vis absorbance spectra, sec 3.3.

Materials and Methods

The practical part of this work involves three stages. The first one is preparing the solution of the six samples with the addition of chlorophyll to the matrix polymer of polymethylmethacrylate in different weight concentrations. The second stage involves the use of the electrospinning technique to produce the samples of nanofibers. The last step is the collection of data on each of the rheological properties, scanning electron microscope (SEM) imaging, and the measurement of the UV-Vis absorbance of the six samples.

The solution of the samples

The magnetic stirrer was the instrument by which the PMMA (the polymer made in Germany by Alpha Chemistry of MW 25000) was dissolved in the solvent acetone at room temperature. The addition of chlorophyll was gradual throughout the polymer solution which lasted for three hours. Table 1, shows at the first line the concentration of the chlorophyll in the solvent of the acetone, and the PMMA. The second line of the table shows the concentration of chlorophyll in the solvent of the PMMA. The solutions were subjected to ultrasonic bathing for twenty minutes to evacuate any potential air bubbles.

Table 1. The addition of chlorophyll was gradual over the duration of the polymer solving which lasted for three hours.

	The Specimens' Concentration (wt.%)					
Chlorophyll in Solution	0	0.05	0.1	0.15	0.2	0.25

Published Online First: September, 2024
https://doi.org/10.21123/bsj.2024.9381
P-ISSN: 2078-8665 - E-ISSN: 2411-7986
Baghdad Science Journal

Chlorophyll in Fibers	0	0.31	0.63	0.94	1.25	1.56

Procedure of electrospinning

During the electrospinning process, many parameters can affect the quality of the fibers produced. However, we focused on the most important parameters that have the biggest impact on stability, such as maintaining a temperature of 25°C, humidity percentage of 5% inside the spinning chamber, a distance of 8 cm between the syringe needle and the earthed collector, a drum rolling speed of 150 rpm, and an applied voltage of 30 kV. We tried to keep the changes between these factors to a minimum to produce high-quality fibers.

Two factors that had a significant impact on the process were the flow rate and the concentration of the fluid used. Generally, we found that as the rate of chlorophyll addition increased, the flow rate required to produce electrospun fibers also increased. For example, the required flow rate for chlorophyll concentrations of 0, 0.05, 0.1, 0.15, 0.2, and 0.25% were 25, 42, 38, 38, 38, and 30 mL/h, respectively. We used an injected solution of 5 mL for each sample to ensure a consistent texture and thickness.

Specimens characterization

The sample characterization was achieved through the measurement or/and analysis of variant solution viscosity by cone plate instrument (made in Germany by Brokfild Co.), FTIR analysis, SEM imaging (the pictures were statistically analyzed by image j software), and UV-Vis absorbance spectra (spectrophotometer, type Shimadzu UV-2450) of 1 nm bandwidth.

Results and Discussion

Rheological properties

The samples were tested for the shear stress versus the shear rate relationship. Fig. 1 uncovers the different behavior of the affected samples by adding variant amounts of chlorophyll.

In accordance with the obtained curves of Fig. 1. it is deduced that Table 2 shows the properties of the different solutions as believed by the parameters of Herschel-Bulkley of fluids.

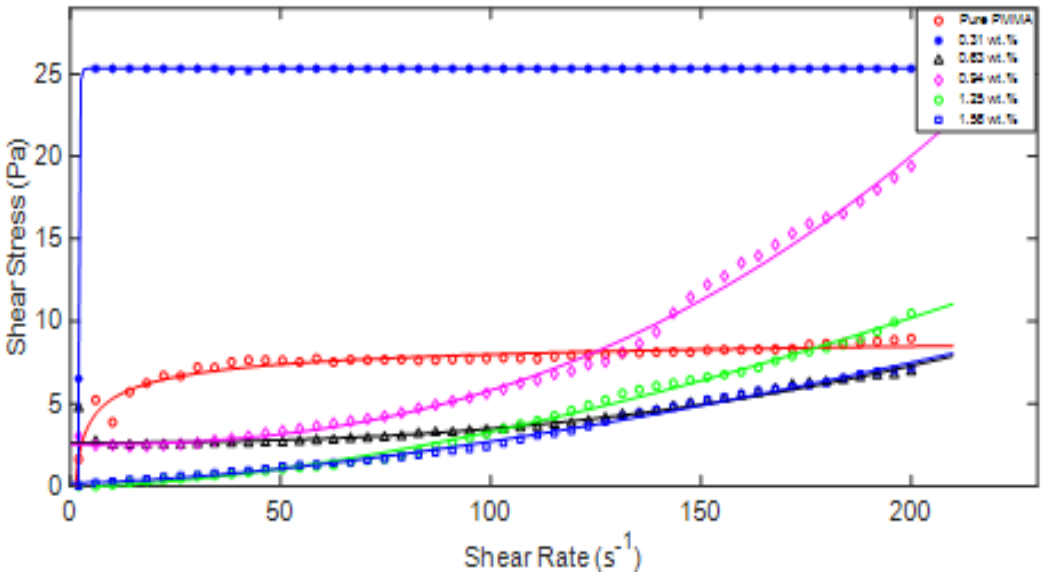

Figure 1. The effect of the additive chlorophyll on the rheological properties of the PMMA solution of concentration 16 wt.%.

Published Online First: September, 2024
https://doi.org/10.21123/bsj.2024.9381
P-ISSN: 2078-8665 - E-ISSN: 2411-7986
Baghdad Science Journal

Table 2. The parameters of Herschel-Bulkley fluid are determined for each concentration of chlorophyll additive in PMMA within micro-nanofibers.

Sample chlorophyll (wt.%)	The yield shear stress (τ_y)	The consistency factor (τ_s)	The flow index (n)
Pure PMMA	10.33	-10.84	-0.33
0.31	25.32	-2.63	-13.77
0.63	2.63	1.1	2.45
0.94	2.52	4.94×10^{-5}	2.41
1.25	0	1.93×10^{-3}	1.62
1.56	0.18	2.15×10^{-3}	1.53

The extracted parameters of the curves' properties are shown in Table 2. In general, all the curves represent Hreschel-Bulkley fluid mathematical formula of Eq. 3 [19].

$$\tau = \tau_y + \tau_s \dot{\gamma}^n \dots\dots\dots\dots\dots\dots\dots\dots\dots\dots 3$$

Where, $\tau, \tau_y, and\ \tau_s$ are the apparent, yield, and surplus shear stress (Pa unit), respectively. $\dot{\gamma}$ is the shear rate (s^{-1} unit). n is the flow index, which refers to the kind of non-Newtonian fluid, whenever, $n < 1$ then the fluid kind of thinning or $n > 1$ then the fluid is thickening. However, for Newtonian fluid $n = 1$. The surplus shear stress τ_s is called the consistency factor as well, due to it relies on the value of the shear rate [20]. It is helpful to recall, that [20] $\tau = \tau_y + \tau_s$. The calculation of the apparent viscosity μ can be done by Eq. 4 [21]:

$$\mu = \frac{\tau}{\dot{\gamma}} \dots\dots\dots\dots\dots\dots\dots\dots\dots\dots\dots\dots 4$$

Then the viscosity is correlated to the apparent shear stress; therefore, the following figure seems beneficial to indicate how the concentration of chlorophyll affects the apparent viscosity of the specimens' solution. Fig. 2 illustrates how fitting a statistical distribution provides insight into its influence.

The progressive value of the chlorophyll concentration in PMMA leads to converting the blend of colloidal to a suspension. Consequently, this change causes a continual decrease in the viscosity [21].

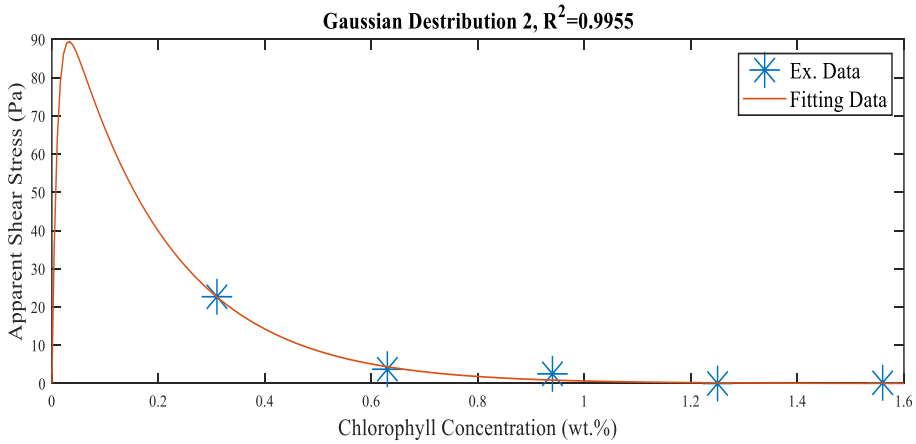

Figure 2. Decreasing the apparent shear stress according to the increasing the chlorophyll concentration. The fitting line shows the obeying the relationship to the Gaussian distribution of the second degree.

Published Online First: September, 2024
https://doi.org/10.21123/bsj.2024.9381
P-ISSN: 2078-8665 - E-ISSN: 2411-7986
Baghdad Science Journal

Images of the SEM

The following step for the stage of obtaining the electrospun fibers was uncovering the quality of the production through imaging by scanning an electronic microscope. Fig. 3 exemplifies the electrospun fibers of the several chlorophyll concentrations have different diameters for each additive weight rate. By using ImageJ software to analyze SEM images, we generated normalized histograms of fiber diameters at varying chlorophyll concentrations. Fig. 4 shows histograms of electrospun fiber diameters for each sample.

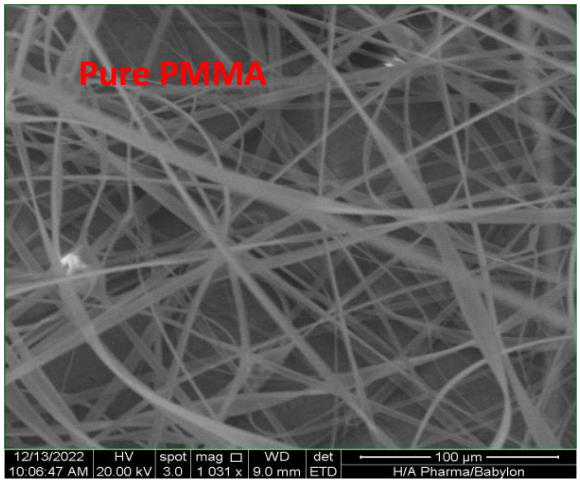

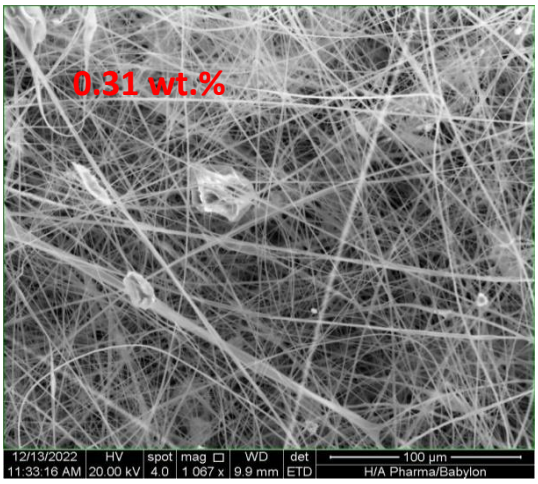

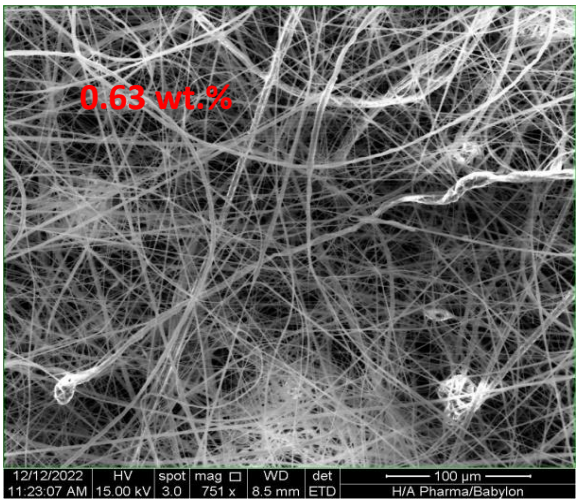

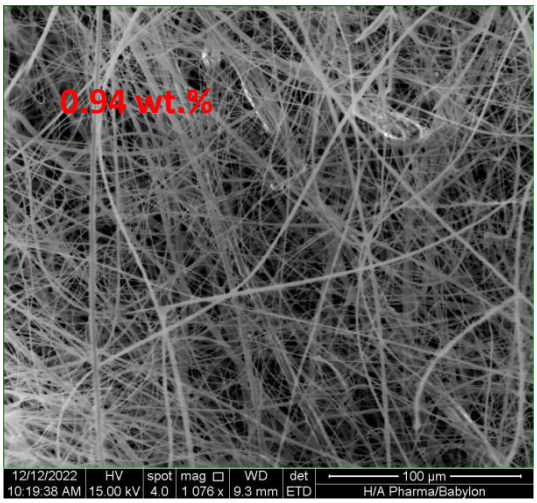

Published Online First: September, 2024
https://doi.org/10.21123/bsj.2024.9381
P-ISSN: 2078-8665 - E-ISSN: 2411-7986
Baghdad Science Journal

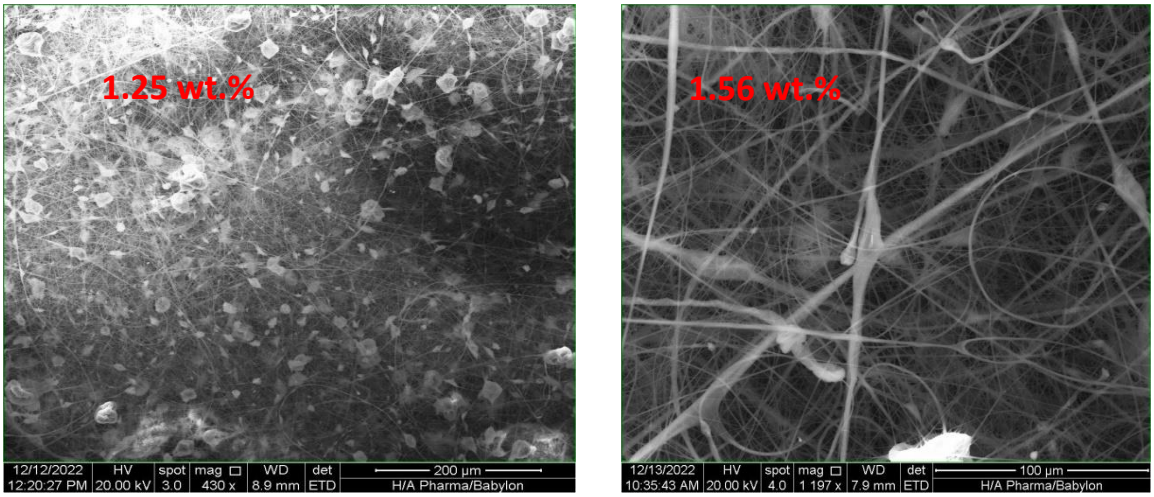

Figure 3. SEM Images of the prepared six specimens of the different chlorophyll concentrations as illustrated on photos.

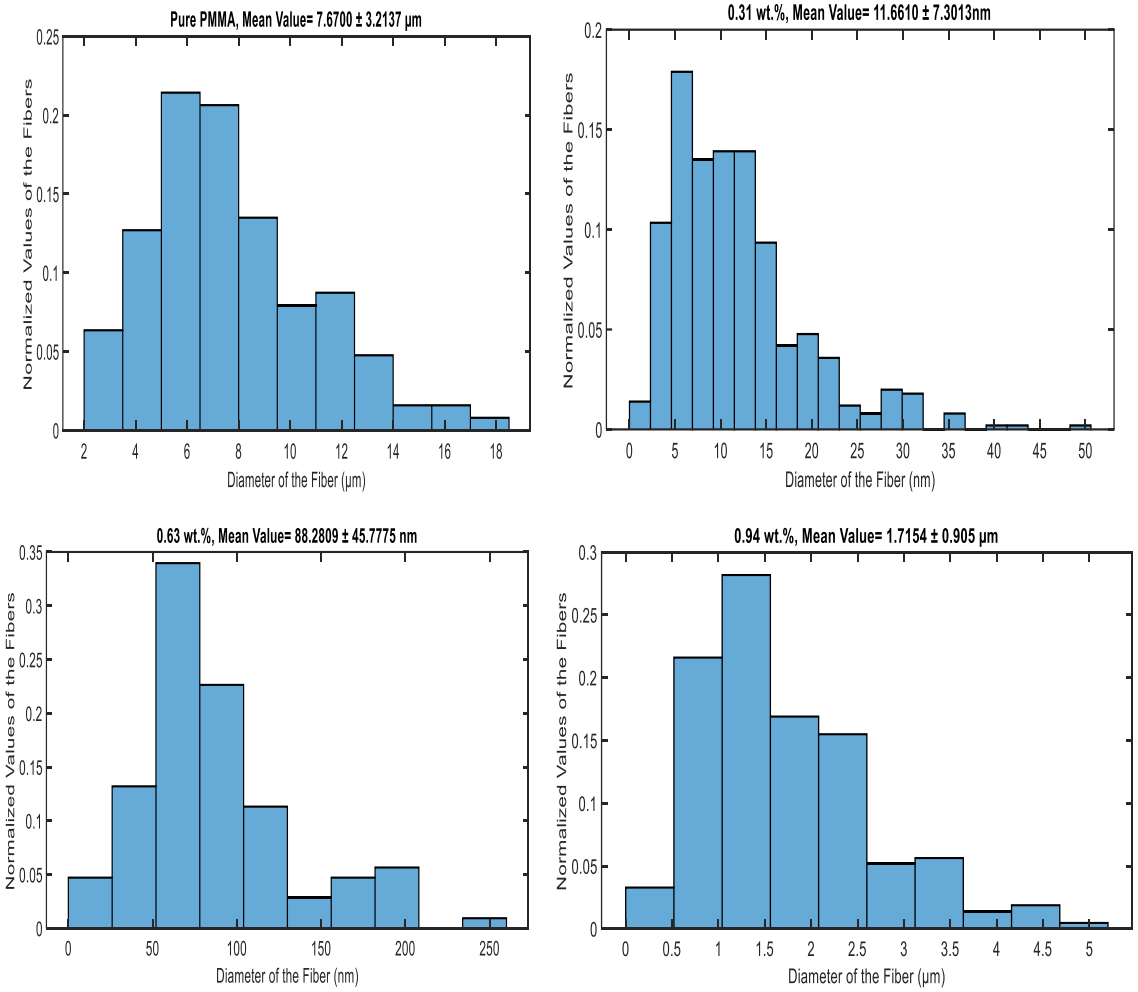

Published Online First: September, 2024
https://doi.org/10.21123/bsj.2024.9381
P-ISSN: 2078-8665 - E-ISSN: 2411-7986
Baghdad Science Journal

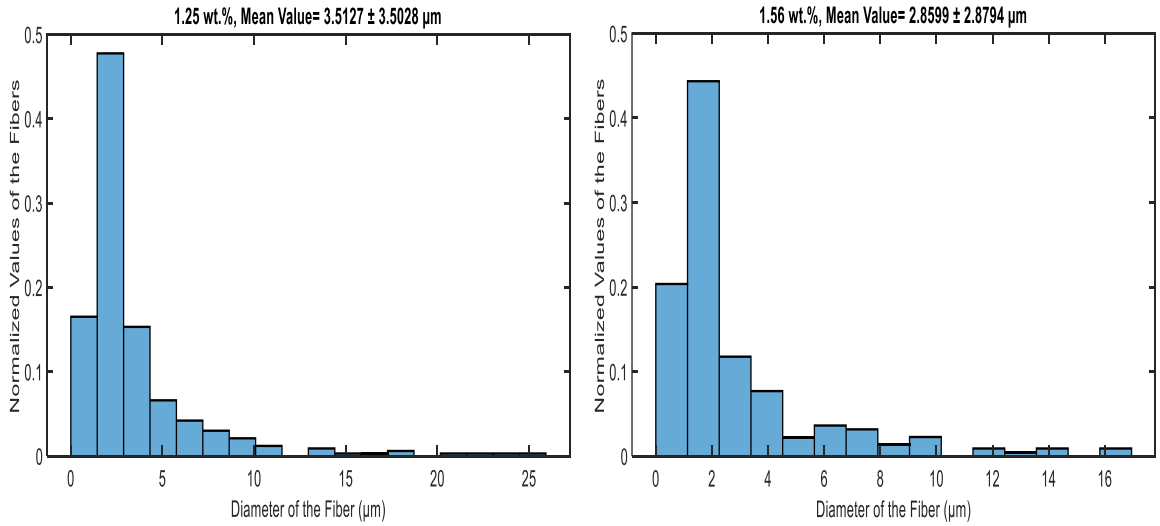

Figure 4. The frequency distribution of the values in a normalized histogram plotted against changes in fiber diameter.

In general, the presence of chlorophyll decreases the diameter of the fibers just nearly for the concentrations of 0.31 wt.% and 0.63 wt.%. Fig. 5 shows that higher chlorophyll concentrations resulted in wider fiber diameter ranges.

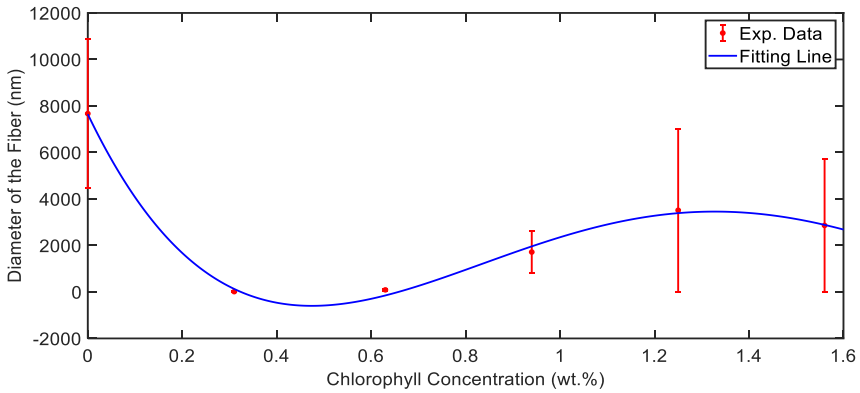

Figure 5. The diameter of fibers changes as the concentration of chlorophyll varies.

The domain of chlorophyll concentration was between ca. 0.2-0.8 wt.% yielding electrospun fibers of concentrated diameter within the range of the nanometer scale. While above this domain, the continual decline of the diameters of the fibers would offer to backfire. The decreasing diameter of fibers the higher the adhesive force between them to create progressively thicker fibers [22]. The bonding by the Van der Waals force makes up bundles of the nanofibers [23]. Dropping the viscosity and the surface tension supports the establishment of not only the backs of thick fibers but also could occur entanglement of the nanofiber to construct beads as it is so obvious in the images of chlorophyll concentrations of 1.25, and 1.56 wt.%. The separated jetting of the electrospinning process, which is controlled by the rheological parameters, causes the contraction of the fibers to be formed as beads as well [24]. Fig. 6 indicates the relationship between the chlorophyll concentration and the standard deviation to mean ratio of fiber diameters, highlighting the dispersion in the dataset.

Published Online First: September, 2024
https://doi.org/10.21123/bsj.2024.9381
P-ISSN: 2078-8665 - E-ISSN: 2411-7986
Baghdad Science Journal

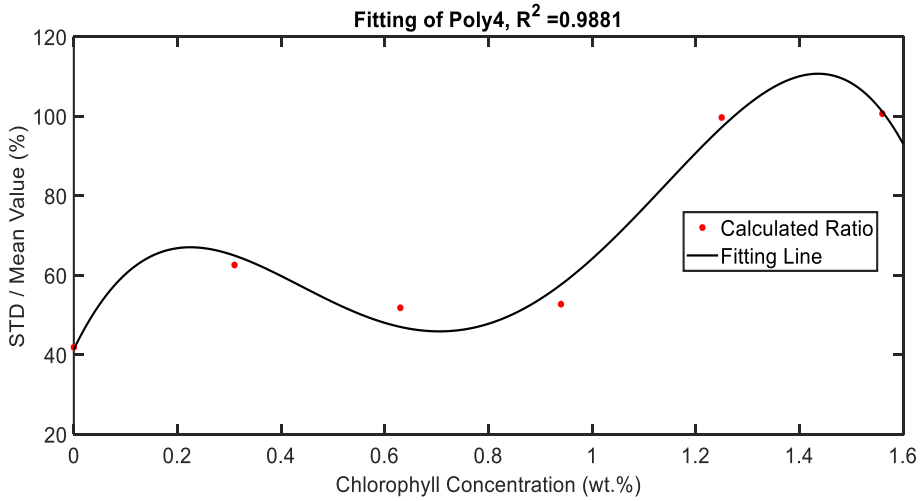

Figure 6. Variation of the diameter spectrum according to the progression values of chlorophyll concentration.

FTIR Analysis

The electrospun fibers were analyzed using FTIR to identify chlorophyll bonding with PMMA. Fig. 7A, B appears bonding of the chlorophyll with the PMMA through the shifting of the wave number for some of the chemical groups of the PMMA.

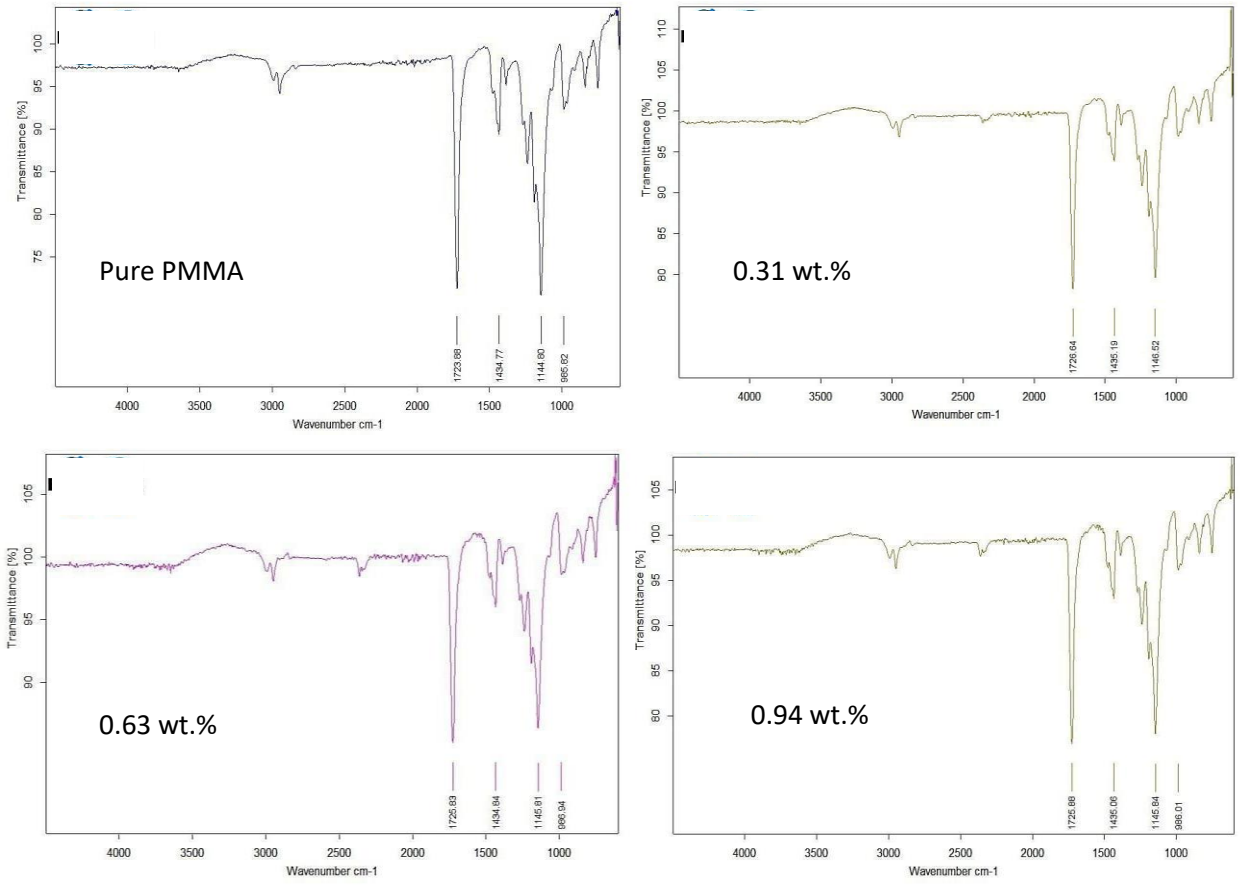

Published Online First: September, 2024
https://doi.org/10.21123/bsj.2024.9381
P-ISSN: 2078-8665 - E-ISSN: 2411-7986
Baghdad Science Journal

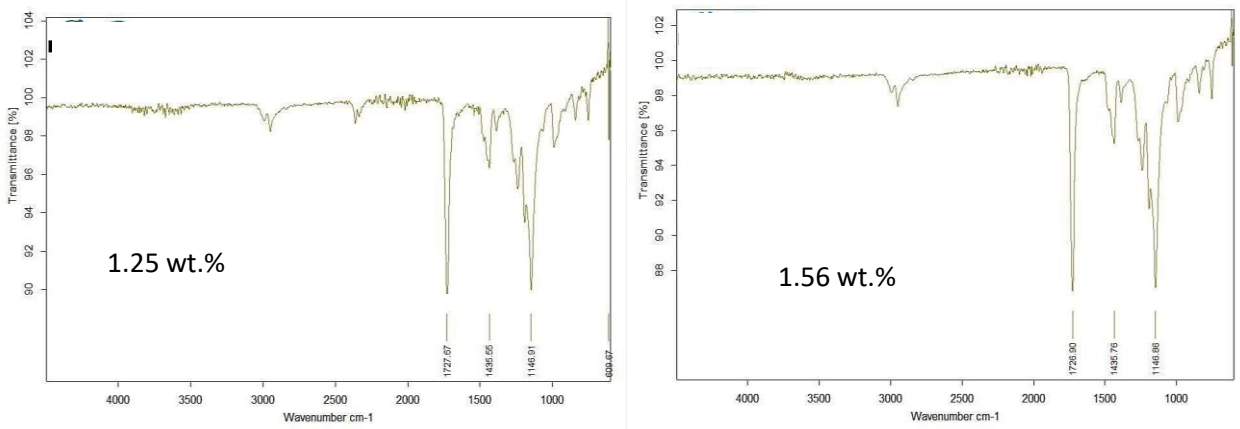

Figure 7A. The FTIR chart of the six samples of different chlorophyll concentrations.

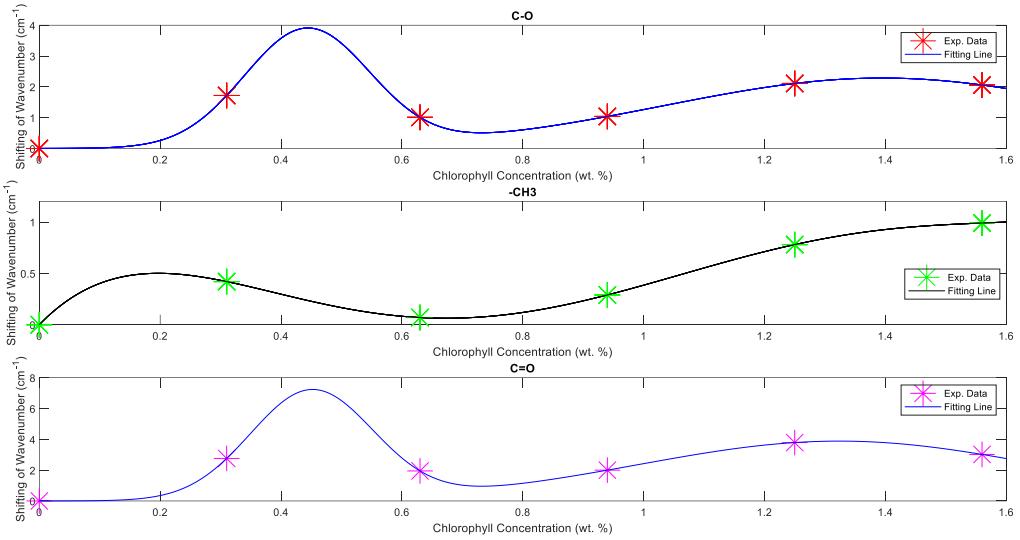

Figure7B. Shifting peaks of FTIR spectra for some chemical groups of the electrospun fibers as statistical distributions by increasing the chlorophyll concentration in the produced micro-nanofibers elucidate the chlorophyll-PMMA physical bonding. As the length of the additive polymer chain increases, the physical bonds between the additive polymer and the matrix polymer can become weaker and more susceptible to elongation [25].

Measurement of UV-vis spectra

Spectra of UV-Vis absorbance

The absorbance measurements of all samples were obtained, and Fig. 8 shows the spectra with error bars at 1 nm intervals. Many prominent points were noted about these spectra, the absorbance was not in direct proportion to the concentration of chlorophyll additive. The rise in absorbance was due to the colloidal nature of the injected solution concentration of 0.31 wt.%. The decline was approximately steady for more increasing chlorophyll concentration that is followed by decreasing the apparent shear stress and viscosity, Fig. 2. The chlorophyll diluted the PMMA and gradually converted the solution into suspensions. Consequently, according to the rheology and the SEM results, that caused a direct increase in the morphological deformation of the texture of the fibers, especially the beads. On top of that, decreasing the surface tension may cause sputtering of the pigment during the jetting process, especially for the concentration of additives of 0.94, 1.25, and 1.56 wt.%.

Published Online First: September, 2024
https://doi.org/10.21123/bsj.2024.9381
P-ISSN: 2078-8665 - E-ISSN: 2411-7986
Baghdad Science Journal

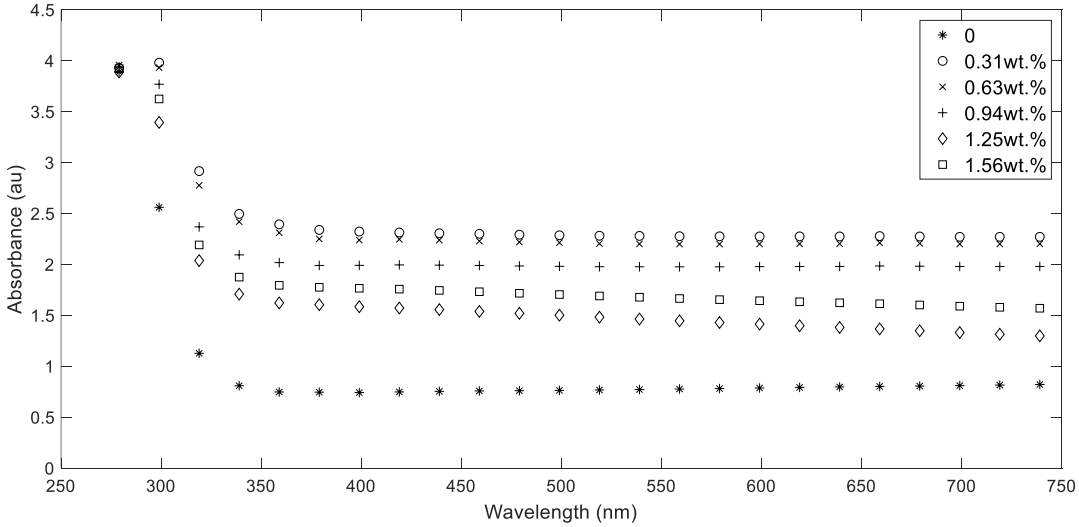

Figure 8. The wavelength-dependent absorbance spectra of the samples were measured for different chlorophyll concentrations.

The absorbance of each sample was calculated for all incident wavelengths and concentrations. Fig. 9 provides a clearer visualization of the radiation screening effect of chlorophyll. Another interesting observation was that the sample of pure PMMA had the highest standard deviation due to the potential synthetic additives. The dispersion of values decreased with increasing chlorophyll pigment in other samples. Fig .10 provides insight into the PMMA structure by analyzing changes in absorbance standard deviation within the samples.

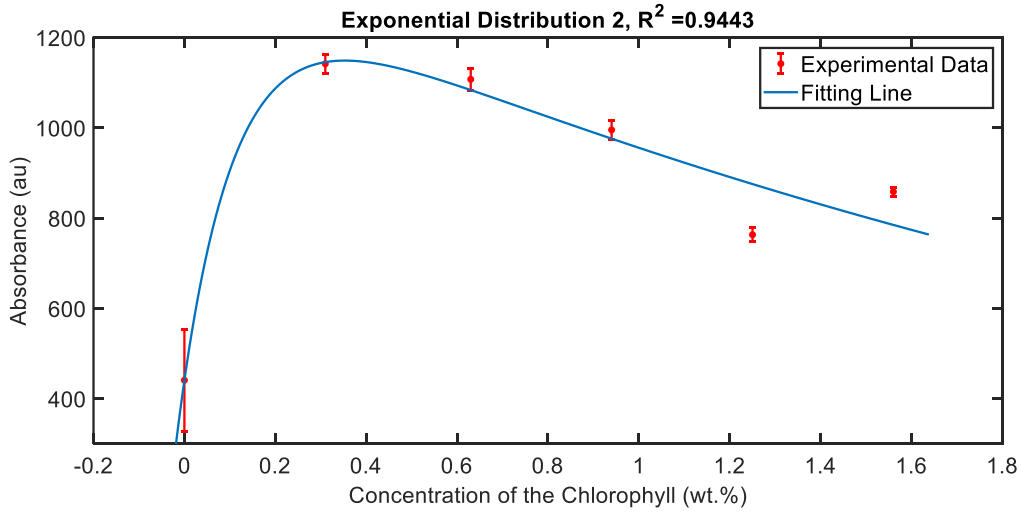

Figure 9. The concentration of chlorophyll is plotted against the total absorbance of each specimen to observe changes.

Published Online First: September, 2024
https://doi.org/10.21123/bsj.2024.9381
P-ISSN: 2078-8665 - E-ISSN: 2411-7986
Baghdad Science Journal

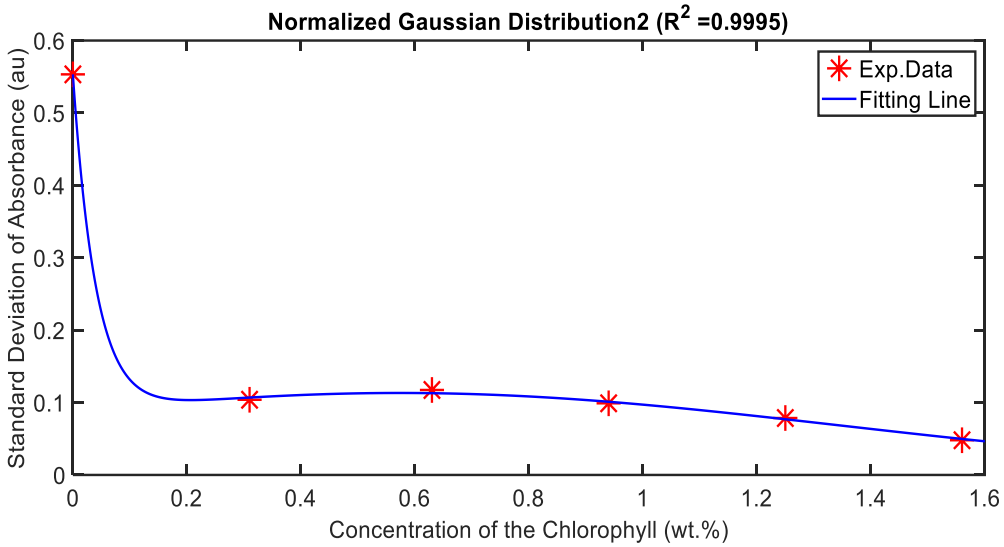

Figure 10. The normalized Gaussian distribution of the change in the standard deviation of absorbance with respect to chlorophyll addition.

Absorption Coefficient

The absorption coefficient is a measure of the amount of light energy absorbed by the intrinsic properties of a material as light passes through it. This concept is different from absorbance, which refers to the attenuation of light passing through a material due to various mechanisms such as scattering, refraction, and absorption [26]. To calculate the absorption coefficient, the thickness of each sample was determined and used in Eq. 1 along with the absorbance value. The value of (t) was measured using the SEM techniques for greater precision. Fig. 11 shows the thickness of the produced electrospun of each sample by using the SEM technique.

The uneven thickness of the samples resulted in a nonlinear effect of the added chlorophyll concentration, Fig. 12 illustrates the change of the absorption coefficient versus the values of the radiation wavelength for each sample.The adhesion mentioned in section 3.2 among the produced fibers caused them to form bundles or coils due to the influence of electric force and increasing aspect ratio to create beads, which led to a thinner texture, and higher density [27].

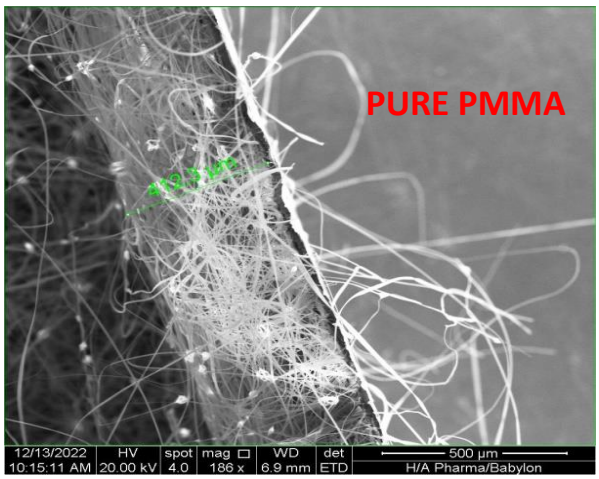

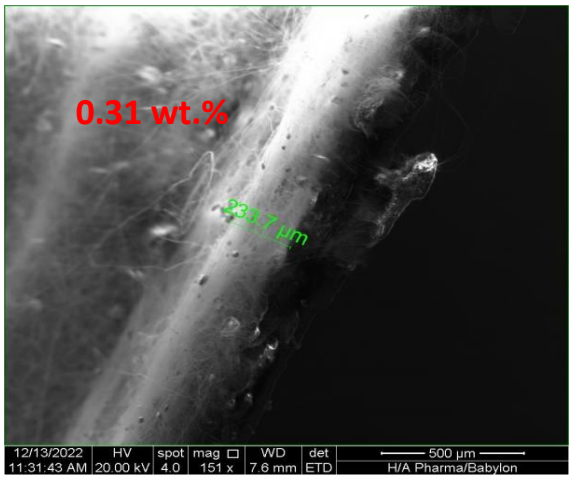

Published Online First: September, 2024
https://doi.org/10.21123/bsj.2024.9381
P-ISSN: 2078-8665 - E-ISSN: 2411-7986
Baghdad Science Journal

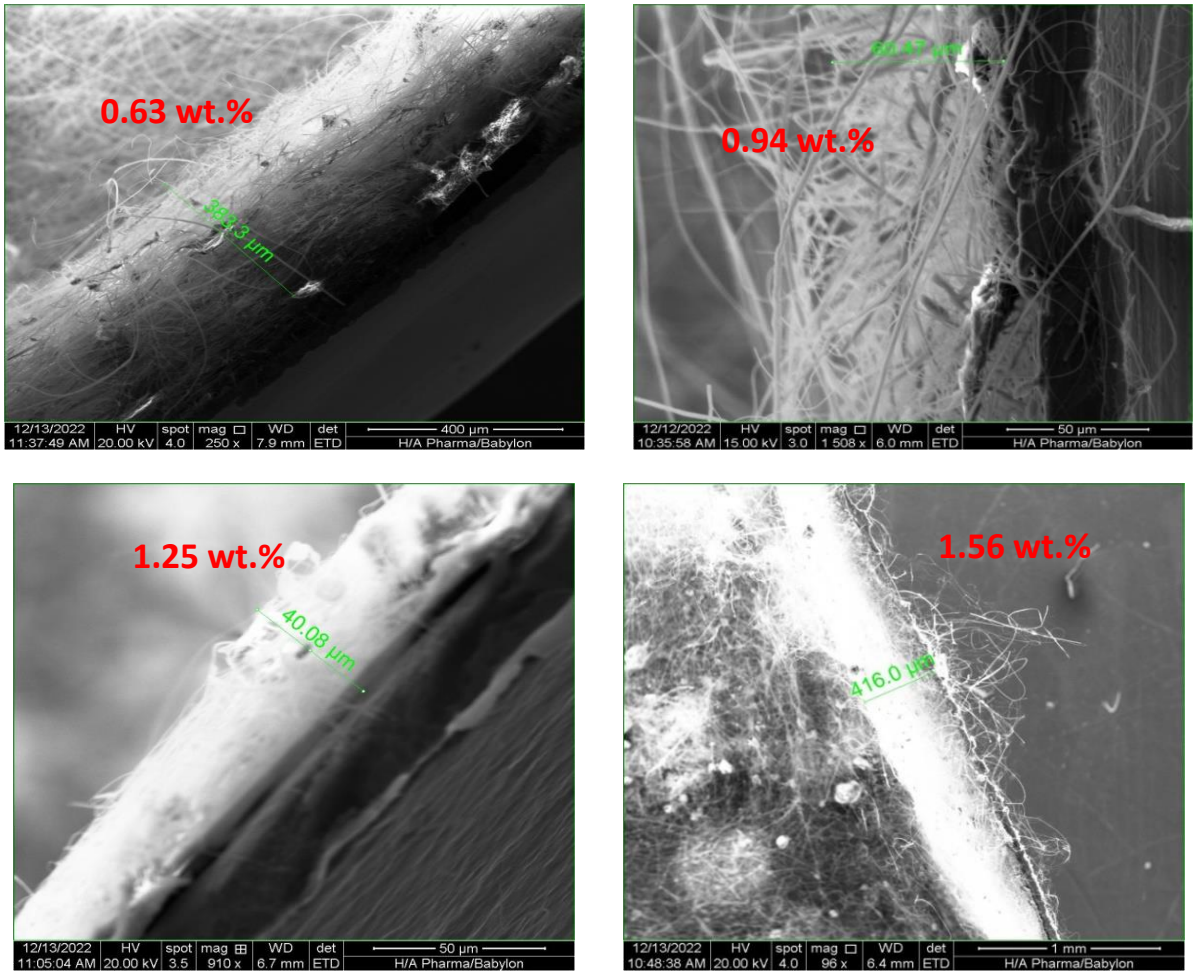

Figure 11. The SEM images of the thickness of the electrospinning fibers produced. Image A shows pure PMMA (402.8 µm), while images B, C, D, E, and F show samples containing chlorophyll concentrations of 0.31 (233.7 µm), 0.63 (383.3 µm), 0.94 (60.47 µm), 1.25 (40.08 µm), and 1.56 (416.0 µm) wt.%, respectively.

This effect was not continuous as it depended on the size of the chlorophyll chain that bonded with PMMA. Fig. 13 explains the fitted line of the change of the absorption coefficient versus the concentration of samples. The Coulomb force is raised by the rise in charge density in the middle of the beads. The action enforced each bead to elongate and push its two halves away. This behaviour turns many of the beads into fibers of different sizes of diameters.

Published Online First: September, 2024
https://doi.org/10.21123/bsj.2024.9381
P-ISSN: 2078-8665 - E-ISSN: 2411-7986
Baghdad Science Journal

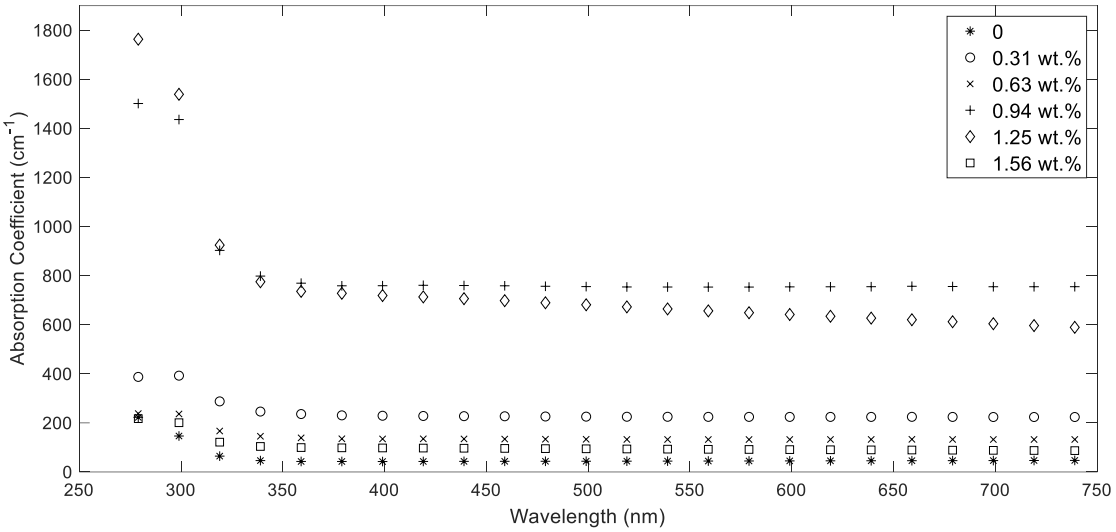

Figure 12. The absorption coefficient changes as the wavelength increases.

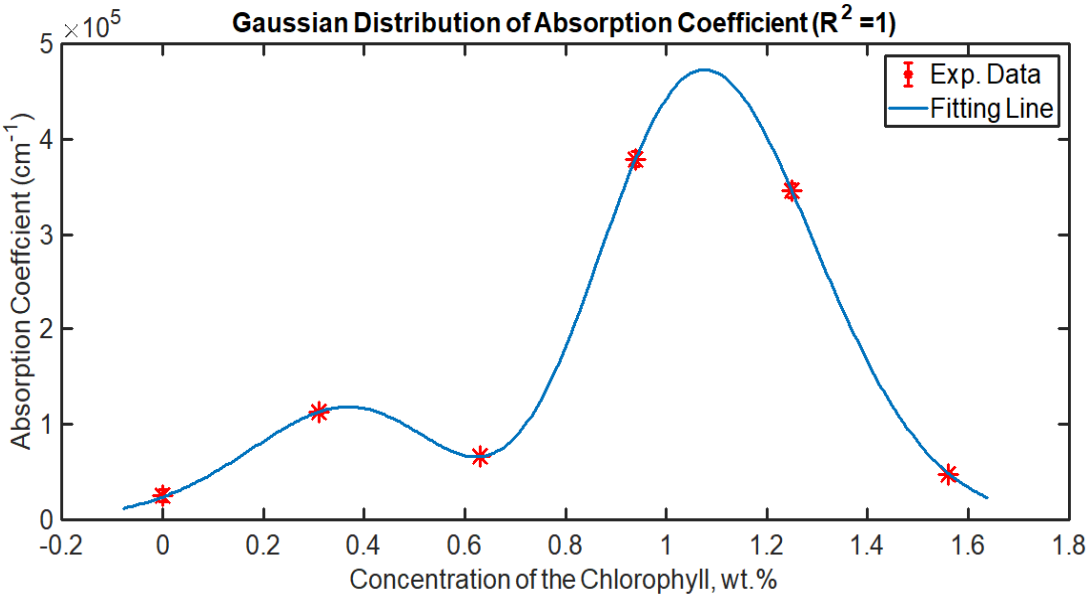

Figure 13. The absorption coefficient of the electrospun fibers follows a Gaussian distribution that depends on the concentration of chlorophyll pigment.

Fig. 14 shows how the standard deviation of the absorption changed according to the variant of the chlorophyll concentration. The notable point is the behaviour corresponding of the absorption coefficient, Figs. 14 and 6. Which referred to a correlation between the diameter of the electrospun fibers and the calculated absorption coefficients. Hear, it is important to recall that the samples were not layers but textures of micro-nanofibers. That means the relationship between the absorbance and/or absorption coefficient is not necessary directly proportional to the concentration. Much lost amount of blend polymer is exposed to the potential entanglements, coiling, sputtering out of the glass substrate. This issue is correlated to the viscosity of the injected solution especially at the concentrations of the chlorophyll of 0.94 and 1.25 wt.%. Fig. 15 shows bead-like images formed due to the hyper-decline of solution viscosity caused by the high concentration of chlorophyll, particularly at 1.25 wt%.

Published Online First: September, 2024
https://doi.org/10.21123/bsj.2024.9381
P-ISSN: 2078-8665 - E-ISSN: 2411-7986
Baghdad Science Journal

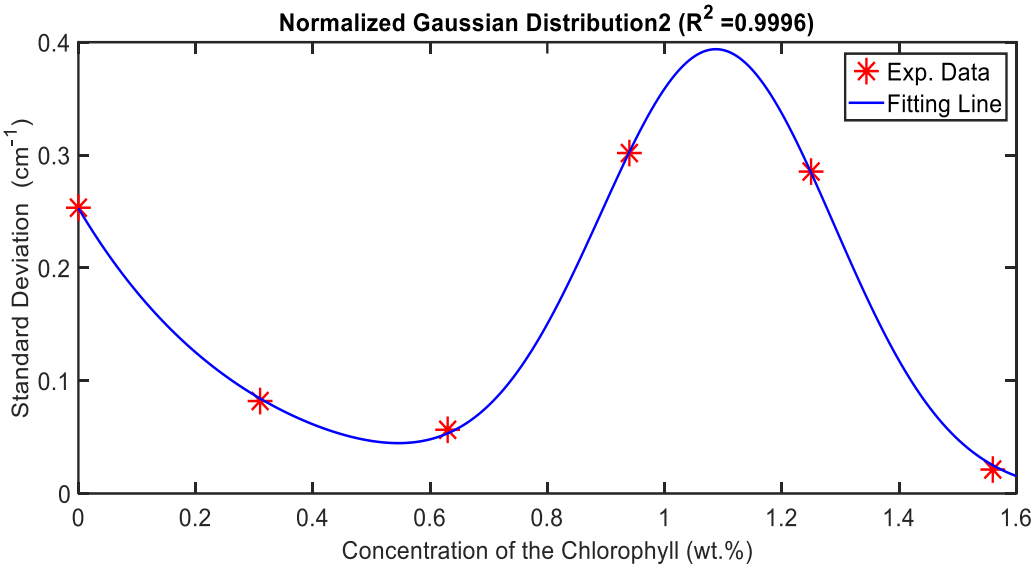

Figure 14. The standard deviation of the absorption coefficient follows a normalized Gaussian distribution over the domain of chlorophyll concentration. High values of the standard deviation may indicate extreme heterogeneity of the sample structure.

Figure 15. Using ImageJ software, a magnified image of a bead (at 200% of Fig. 4, 1.25 wt. %) shows an entanglement of fibers.

Calculation of Energy Gap

The energy gap was determined by Tauc's method [28], using the absorbance data. Fig. 16 shows how the band gap was determined using two optical measurements for each sample at different orientations.

Published Online First: September, 2024
https://doi.org/10.21123/bsj.2024.9381
P-ISSN: 2078-8665 - E-ISSN: 2411-7986
Baghdad Science Journal

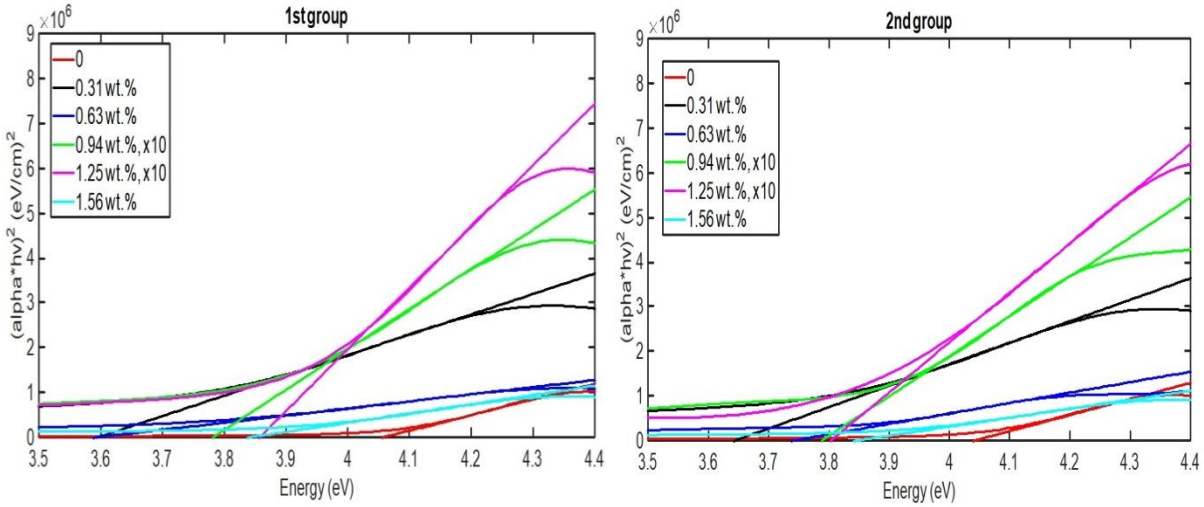

Figure 16. The two measurements of the same samples under the names of group one and group two. The band gaps were calculated for the several chlorophyll concentrations.

It is clear; the energy gap values do not change linearly depending on the enlargement of the chlorophyll concentration in the obtained micro-nanofibers. Fig. 17 shows the relationship between band gap values and chlorophyll concentration. However, it is an indicator of the extent of the overlapping between the components of the polymeric blend [29]. The band gap represents the amount of required energy for an electron to transit from HOMO to the LUMO band. The band gab value is contracting in the cases of blends with high compatibility among the components of it and vice versa.

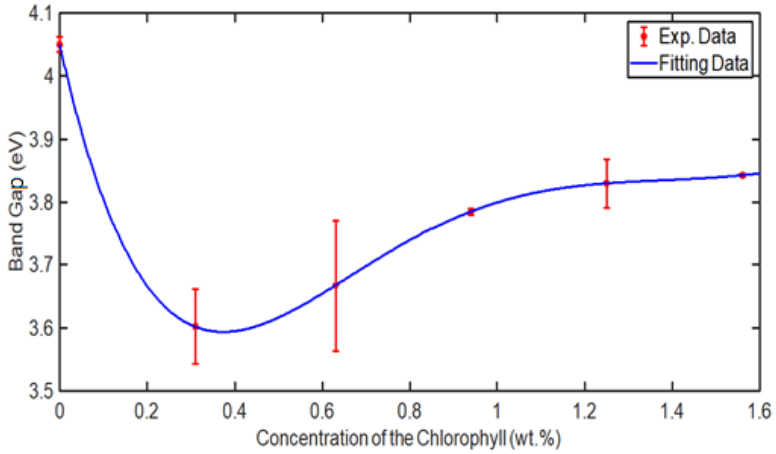

Figure 17. The nonlinear relationship of the band gab values of the PMMA samples of different chlorophyll concentration versus the values of the chlorophyll concentration.

The non-linear effect of the pigment on the band gap value of the host polymer depends on the natural interaction of the two polymeric species of the blend [30]. The concentration and the chemical structure of the pigment play an essential role in the reconfiguration of the energy states of the blend. In accordance with these alterations the absorption, and reflection of the incident light wavelength on the material is quantified. However, the band gap value of the PMMA is 3.6-4.2 eV [31]. that it depends on the doping concentration and the measurement method [32-34].

Published Online First: September, 2024
https://doi.org/10.21123/bsj.2024.9381
P-ISSN: 2078-8665 - E-ISSN: 2411-7986
Baghdad Science Journal

Conclusion

The study reveals how chlorophyll concentration affects the properties of electrospun PMMA/chlorophyll nanofibers. The results show that the viscosity of the blend solution determines the morphology and quality of the nanofibers. The optimal chlorophyll concentration produces uniform and bead-free nanofibers. The study also proposes a new theoretical framework for explaining the optical properties of the nanofibers. The results show that the band gap of the nanofibers increases with chlorophyll concentration, making them more suitable for applications such as solar cells and LEDs. Moreover, the study shows that the surface roughness of the nanofibers increases with chlorophyll concentration, which could be beneficial for applications such as tissue engineering and water filtration. The study provides a comprehensive and theoretical understanding of the relationship between chlorophyll concentration and the properties of electrospun PMMA/chlorophyll nanofibers, which is essential for the design and development of new and improved nanofiber-based materials.

Newly Formulated Theoretical Contributions

The study makes the following new theoretical contributions:

- Optimal chlorophyll concentration for producing high-quality and uniform nanofibers.
- New theoretical framework for understanding the optical properties of the nanofibers.
- Role of chlorophyll concentration in determining the surface properties of the nanofibers.

Acknowledgment

Special words of thanks to Dr. Mazen Jaafar, Dr. Haider Obeis (Pharmacy College / University of Babylon), Dr. Ahmed Hashim (College of Education for Pure Science), and Ms. Duha (College of Materials Engineering) for their assistance.

Authors' Declaration

- Conflicts of Interest: None.
- We hereby confirm that all the Figures and Tables in the manuscript are ours. Furthermore, any Figures and images, that are not ours, have been included with the necessary permission for re-publication, which is attached to the manuscript.
- No animal studies are present in the manuscript.
- No human studies are present in the manuscript.
- Ethical Clearance: The project was approved by the local ethical committee at University of Babylon.

Authors' Contribution Statement

Z.A. financed and performed the experimental part. M.A. designed and wrote the manuscript.

References

1. Jahan I, Zhang L. Natural Polymer-Based Electrospun Nanofibrous Membranes for Wastewater Treatment: A Review. J Polym Environ. 2022 Nov; 30 (4): 1709–1729. https://doi.org/10.1007/s10924-021-02312-1.
2. Tahir M, Vicini S, Sionkowska A. Electrospun Materials Based on Polymer and Biopolymer Blends— Rev. Polym. 2023 Mar; 15(7): 1654. https://doi.org/10.3390/polym15071654.
3. Khadayeir AA, Wannas AH, Yousif FH. Effect of Applying Cold Plasma on Structural, Antibacterial and Self Cleaning Properties of α-Fe2O3 (HEMATITE) Thin Film. Emerg Sci J. 2022 Feb; 6(1): 75-85. https://doi.org/10.28991/ESJ-2022-06-01-06.
4. Hosseini SM, Esmaeili M. PMMA/chlorophyll composite nanofibrous membranes for the removal of heavy metals from water. J Water Process Eng. 2021

Published Online First: September, 2024
https://doi.org/10.21123/bsj.2024.9381
P-ISSN: 2078-8665 - E-ISSN: 2411-7986
Baghdad Science Journal

Dec; 41(12): 1-10. https://doi.org/10.1016/j.jwpe.2021.102084.
5. Nworie FS, Mgbemena N, Ike-Amadi AC, Ebunoha J. Functionalized Biochars for Enhanced Removal of Heavy Metals from Aqueous Solutions: Mechanism and Future Industrial Prospects. J Hum Earth Future. 2022 Sep; 3(3): 1-10. https://doi.org/10.28991/HEF-2022-03-03-09.
6. Ratnawati R, Wulandari R, Kumoro AC, Hadiyanto H. Response Surface Methodology for Formulating PVA/Starch/Lignin Biodegradable Plastic. Emerg Sci J. 2022 Apr; 6(2): 1-10. https://doi.org/10.28991/ESJ-2022-06-02-03.
7. Wang M, Wang K, Yang Y, Liu Y, Yu D-G. Electrospun Environment Remediation Nanofibers Using Unspinnable Liquids as the Sheath Fluids: Rev Polym. 2020 Jan; 12(1):103. https://doi.org/10.3390/polym12010103.
8. Ince Yardimci A, Yagmurcukardes N, Yagmurcukardes M, et al. Electrospun polyacrylonitrile (PAN) nanofiber: preparation, experimental characterization, organic vapor sensing ability and theoretical simulations of binding energies. Appl Phys A; 2022 Feb; 128 (2): 173. https://doi.org/10.1007/s00339-022-05314-5.
9. Wang H, Liu Q, Yang Q, Li Y, Wang W, Sun L, et al. Electrospun poly(methyl methacrylate) nanofibers and microparticles. J Mater Sci; 2010 Feb; 45 (3): 1032–1038. https://doi.org/10.1007/s10853-009-4035-1.
10. Maliszewska I, Czapka T. Electrospun Polymer Nanofibers with Antimicrobial Activity. Polym. 2022 Apr; 14(9): 1661. https://doi.org/10.3390/polym14091661.
11. Liu R, Hou L, Yue G, Li H, Zhang J, Liu J, et al. Progress of Fabrication and Applications of Electrospun Hierarchically Porous Nanofibers. Adv Fiber Mater. 2022; 4 (4): 604–630. https://doi.org/10.1007/s42765-022-00132-z
12. Cao X, Chen W, Zhao P, Yang Y, Yu D-G. Electrospun Porous Nanofibers: Pore−Forming Mechanisms and Applications for Photocatalytic Degradation of Organic Pollutants in Wastewater. Polym. 2022; 14(19): 3990. https://doi.org/10.3390/polym14193990.
13. Odularu AT. Basic principles of electrospinning, mechanisms, nanofibre production, and anticancer drug delivery. J Chem. 2022 Apr; 2022(1):1-16. https://doi.org/10.1155/2022/9283325.
14. Cherubin A, Destefanis L, Bovi M, Perozeni F, Bargigia I, de la Cruz Valbuena G. Encapsulation of photosystem I in organic microparticles increases its photochemical activity and stability for ex vivo photocatalysis. ACS Sustain Chem Eng. 2019 May; 7(12): 10435–44. https://doi.org/10.1021/acssuschemeng.9b00738.
15. Shanshool HM, Yahaya M, Yunus WMM, Abdullah IY. Investigation of energy band gap in polymer/ZnO nanocomposites. J Mater Sci Mater Electron. 2016 May; 27(11): 9804–9811. https://doi.org/10.1007/s10854-016-5046-8.
16. Mahmoud RK, Taha M, Zaher A, Amin RM. Understanding the physicochemical properties of Zn–Fe LDH nanostructure as sorbent material for removing of anionic and cationic dyes mixture. Sci Rep. 2021 Nov; 11(1): 1-11. https://doi.org/10.1038/s41598-021-00437-w.
17. Abdul Jabbar GAH, Saeed AA, Hadi AL-Kadhemy MF. Optical characteristics and bacterial-resistance ability of PVA/ZnO nanocomposites. Kuwait J Sci. 2023 Jul; 50(3): 209–2015. https://doi.org/10.1016/j.kjs.2023.03.004.
18. Khalil MM, El-Sayed AH, Masoud MS, Mahmoud EM, Hamad MA. Synthesis and optical properties of alizarin yellow GG-Cu (II)-PVA nanocomposite film as a selective filter for optical applications. J Mater Res Technol. 2021 Apr; 11(1): 33–39. https://doi.org/10.1016/j.jmrt.2021.01.102.
19. Denkov N, Tcholakova S, Politova-Brinkova N. Physicochemical control of foam properties. Curr Opin Colloid Interface Sci. 2020 Dec; 50(6): 101376. https://doi.org/10.1016/j.cocis.2020.08.001.
20. Amin A-TM, Hamzah WAW, Oumer AN. Thermal conductivity and dynamic viscosity of mono and hybrid organic-and synthetic-based nanofluids: A critical review. Nanotechnol Rev. 2021 Jan; 10(1): 1624–61. https://doi.org/10.1515/ntrev-2021-0086.
21. Sajjad M, Otsuki A. Coupling flotation rate constant and viscosity models. RSC Adv. 2022; 12(3): 409-417. https://doi.org/10.3390/met12030409.
22. Sun Y, Cheng S, Lu W, Wang Y, Zhang P, Yao Q. Electrospun fibers and their application in drug controlled release, biological dressings, tissue repair, and enzyme immobilization. RSC Adv. 2019 Dec; 9(44): 25712–25729. https://doi.org/10.3390/polym11122008.
23. Meyer M, Buchberger G, Heitz J, Baiko D, Joel A-C. Ambient Climate Influences Anti-Adhesion between Biomimetic Structured Foil and Nanofibers. Nanomaterials. 2021 Nov; 11(12): 3222. https://doi.org/10.3390/nano11123222.
24. Saad EM, El Gohary NA, El-Shenawy BM, Handoussa H, Klingner A, Elwi M. Fabrication of magnetic molecularly imprinted beaded fibers for rosmarinic acid. Nanomaterials. 2020 Jul; 10(8): 1478. https://doi.org/10.3390/nano10081478.
25. Gabriele PD, Geib JR, Puglisi JS, Reid WJ. Photochemical Degradation and Biological Defacement of Polymers — I. In: Kresta JE, editor.

Published Online First: September, 2024
https://doi.org/10.21123/bsj.2024.9381
P-ISSN: 2078-8665 - E-ISSN: 2411-7986
Baghdad Science Journal

Polymer Additives. Polym Sci Technol, 1984; 26: 83–106. https://doi.org/10.1007/978-1-4613-2797-4_5.
26. Sillanpaa M, Park Y. Natural Organic Matter in Water: Characterization, Treatment Methods, and Climat Change Impact. Butterworth-Heinemann. 2022 Oct; 26. https://doi.org/10.1016/C2018-0-01701-9.
27. Puppi D, Pecorini G, Chiellini F. Biomedical processing of polyhydroxyalkanoates. Bioeng. 2019 Nov; 6(4): 108. https://doi.org/10.3390/bioengineering6040108.
28. Makuła P, Pacia M, Macyk W. How to correctly determine the band gap energy of modified semiconductor photocatalysts based on UV–Vis spectra. J Phys Chem Lett. 2018 Dec; 9(28): 6814–6817. https://doi.org/10.1021/acs.jpclett.8b02892.
29. Aziz SB, Marif RB, Brza MA, Hassan AN, Ahmad HA. Structural, thermal, morphological and optical properties of PEO filled with biosynthesized Ag nanoparticles: New insights to band gap study. Results Phys. 2019 Jun; 13: 102220. https://doi.org/10.1016/j.rinp.2019.102220.
30. Kumari LS, George G, Rao PP, Reddy MLP. The synthesis and characterization of environmentally benign praseodymium-doped TiCeO4 pigments. Dyes Pigm. 2008 May; 77(2): 427–31. https://doi.org/10.1016/j.dyepig.2007.07.007.
31. Ismail LN, Zulkefle H, Herman SH, Rusop Mahmood M. Influence of doping concentration on dielectric, optical, and morphological properties of PMMA thin films. Adv Mater Sci Eng. 2012 Feb; 2012: 5. https://doi.org/10.1155/2012/605673.
32. Al-Bataineh QM, Ahmad AA, Alsaad AM, Telfah AD. Optical characterizations of PMMA/metal oxide nanoparticles thin films: bandgap engineering using a novel derived model. Heliyon. 2021Jan; 7(1): e05952. https://doi.org/10.1016/j.heliyon.2021.e05952.
33. Akraa MA, Hasan AS, Kadhim MH. Spectroscopy Characterization of Ethylene Vinyl Acetate Degradation by Different Kinds of Accelerated Aging. Baghdad Sci J. 2020 Sep; 17(3): 795-805. https://doi.org/10.21123/bsj.2020.17.3.0795.
34. Alkarbouly SM, Waisi BI. Fabrication of Electrospun Nanofibers Membrane for Emulsified Oil Removal from Oily Wastewater. Baghdad Sci. J. 2022 Dec; 19(6): 1238-1248. https://doi.org/10.21123/bsj.2022.6421.

تأثير تركيز الكلوروفيل على إنتاج ألياف أكريليك نانوية بتقنية الغزل الكهربائي

زينب جاسم الحسيني، محمد عبد الحمزة اكرع

قسم الفيزياء، كلية التربية للعلوم الصرفة، جامعة بابل، حله، العراق.

الخلاصة

تستكشف هذه الدراسة خصائص الألياف النانوية المغزولة كهربائيًا من بولي ميثيل ميثاكريلات (PMMA) الممزوجة بالكلوروفيل، والتي من الممكن تطبيقها في تصنيع الخلايا الكهروضوئية. تمت إضافة تراكيز مختلفة من الكلوروفيل (0، 0.05، 0.1، 0.15، 0.2، و0.25 بالوزن%) إلى محاليل الغزل الكهربائي لـ PMMA والأسيتون. بعد عملية الغزل الكهربائي وتبخر الأسيتون، احتوت الألياف على تراكيز الكلوروفيل (0، 0.31، 0.63، 0.94، 1.25، و1.56 بالوزن%). تم توصيف الالياف المنتجة بخصائص الريولوجيا، وتحول فوريه بالأشعة تحت الحمراء، والمجهر الإلكتروني الماسح، والتحليل الطيفي للأشعة فوق البنفسجية. أظهرت النتائج أن الكلوروفيل زاد من لزوجة المحلول وقلل من قطر الألياف النانوية بنسبة وزنية تصل إلى 0.8%. تم الحصول على الألياف النانوية الأكثر اتساقًا بنسبة وزنية تبلغ 0.31% من الكلوروفيل، بمتوسط قطر 11.66 ± 7.3 نانومتر. أدت تركيزات الكلوروفيل الأعلى إلى ألياف نانوية أكبر وأكثر انتظامًا وزيادة فجوة النطاق. أنتجت تراكيز الكلوروفيل التي تزيد عن 1% بالوزن أليافًا غير مرغوب فيها ذات خرز. حددت الدراسة النطاق الأمثل لتركيز الكلوروفيل في ألياف PMMA النانوية (0-0.8 بالوزن%) ودرست تأثير الكلوروفيل على اللزوجة والقطر وفجوة النطاق ومورفولوجيا الألياف النانوية. توفر الدراسة معلومات مفيدة للباحثين والمطورين الذين يرغبون في استخدام ألياف PMMA/الكلوروفيل النانوية لأغراض مختلفة.

الكلمات المفتاحية: صبغة الكلوروفيل، الغزل الكهربائي، الألياف النانوية المغزولة بالكهرباء، ذوبان البوليمر، محلول البوليمر.